

# Preparation of Ag-Fe<sub>3</sub>O<sub>4</sub> nanoparticles sensor and application in detection of methomyl

Ke Gai<sup>1,2</sup>, Huili Qi<sup>2</sup>, Xiulan Zhu<sup>1,\*</sup>, and Mingye Wang<sup>2</sup>

<sup>1</sup>Longdong University, College of Energy Engineering, Qingyang745000, China

<sup>2</sup>Long Dong University, College Chemistry & Chemical Engineering, Qingyang745000, China

**Abstract.** Ag-doped Fe<sub>3</sub>O<sub>4</sub> nanoparticles (Ag-Fe<sub>3</sub>O<sub>4</sub>) was successfully synthesized by the hydrothermal method and performed a simple chemical reaction process in a significantly shorter time than traditional solvothermal method. Furthermore, Ag-Fe<sub>3</sub>O<sub>4</sub> electrochemical sensor was prepared using chitosan and acetic acid as crosslinkers, and the electrochemical behavior of methomyl on the electrode was studied by cyclic voltammetry. Experimental results showed that the electrode had faster response, higher detection sensitivity and better stability for methomyl. Under optimal conditions, the linear current response was achieved in the concentration range of  $2.97 \times 10^{-5} \text{ mol} \cdot \text{L}^{-1} \sim 3.47 \times 10^{-4} \text{ mol} \cdot \text{L}^{-1}$ , with the detection limit of  $2.08 \times 10^{-5} \text{ mol} \cdot \text{L}^{-1}$ . The methomyl in different vegetable samples was detected, and its recovery rate was between 90%~98%.

## 1 Introduction

Carbamate pesticides are synthetic pesticides developed after organophosphorus pesticides. Because of its characteristics of strong selectivity, high efficiency, broad spectrum, low toxicity to humans and livestock, easy decomposition and low residual toxicity, it has been widely used in agriculture, forestry, and animal husbandry. However, large amounts of residual carbamate pesticides remain in the environment, and lead to serious water pollution. Residual pesticides entered the human bodies along with the food chain. As a result, cholinesterase activity could be inhibited and the hydroxyl group of serine in the enzyme active center could be carbamylated. More seriously, enzymes would lose the hydrolysis ability of acetylcholine and cause poisoning due to the accumulation of acetylcholine in the tissues. Even cholinergic characteristic of tears, salivation, pupils dilate, convulsions and death would occur. Therefore, residues of carbamate pesticides are detected timely and accurately, which is of great importance in developing and using pesticides rationally, and protecting the ecological environment and human health.

Traditional detecting methods of residual pesticides include high performance liquid chromatography [1], gas chromatography/mass spectroscopy [2], spectrophotometry [3], chemiluminescence [4] and enzymatic inhibition method [5]. Although these methods can accurately detect content of residual pesticides, the equipment is expensive and the sample pretreatment methods are tedious with long analysis

period. Recently, with the rapid development of electrochemical sensing technology, more researchers are committed to developing a rapid, sensitive and simple carbamate pesticide sensor used in on-site monitoring.

Magnetic Fe<sub>3</sub>O<sub>4</sub> nanoparticles have good biocompatibility. Their special electronic configuration and chemical bonding activity are applied to biosensors such as immune sensors and DNA sensors to promote the electron transport. Recently, a lot of work has been done to modify the surface of Fe<sub>3</sub>O<sub>4</sub> nanoparticles to produce different kinds of composite nanoparticles in many experiments. The present paper shows the nanosilver-doped magnetic Fe<sub>3</sub>O<sub>4</sub> nanoparticles could improve the stability of nanoparticles and the synthesized Ag-Fe<sub>3</sub>O<sub>4</sub> nanoparticles was applied to the preparation of electrochemical sensors. Therefore, a method for detecting carbamate residual pesticides was established.

Methomyl is an N-methyl carbamate saccharide insecticide of all carbamate pesticides. In this paper, Ag-Fe<sub>3</sub>O<sub>4</sub>/GCE (glassy carbon electrode) chemical sensor was constructed by the characteristics of Ag-Fe<sub>3</sub>O<sub>4</sub> composites, and its electrochemical behavior of methomyl on the electrode was measured for further measuring the carbamate pesticide residues in agricultural products.

## 2 Experimental Section

### 2.1 Materials

Disodium hydrogen phosphate (Na<sub>2</sub>HPO<sub>4</sub>), sodium dihydrogen phosphate (NaH<sub>2</sub>PO<sub>4</sub>), sodium hydroxide (NaOH), iron sulfate (Fe<sub>2</sub>(SO<sub>4</sub>)<sub>3</sub>), ferrous sulfate (FeSO<sub>4</sub>),

\* Corresponding author: Xiulan Zhu, [keazhuk@126.com](mailto:keazhuk@126.com)

sulfuric acid ( $\text{H}_2\text{SO}_4$ ), trisodium citrate ( $\text{C}_6\text{H}_5\text{Na}_3\text{O}_7 \cdot 2\text{H}_2\text{O}$ ), sodium dodecylbenzene sulfonate ( $\text{C}_{18}\text{H}_{29}\text{NaO}_3\text{S}$ ), silver nitrate ( $\text{AgNO}_3$ ), soluble starch ( $\text{C}_{12}\text{H}_{22}\text{O}_{11}$ ), glucose ( $\text{C}_6\text{H}_{12}\text{O}_6$ ), ferricyanide Potassium ( $\text{K}_3[\text{Fe}(\text{CN})_6]$ ), potassium nitrate ( $\text{KNO}_3$ ), chitosan ( $(\text{C}_6\text{H}_{11}\text{NO}_4)_n$ ), absolute ethanol ( $\text{C}_2\text{H}_5\text{OH}$ ), methomyl ( $\text{C}_5\text{H}_{10}\text{N}_2\text{O}_2\text{S}$ , 20%), phoxim ( $\text{C}_{12}\text{H}_{15}\text{N}_2\text{O}_3\text{PS}$ ) and dichlorvos ( $\text{C}_4\text{H}_7\text{Cl}_2\text{O}_4\text{P}$ ) were all used in this study, and these chemicals were commercially available and of analytical grade. The ultra-pure water was used. Spinach, oilseed rape and lettuce was purchased from the backdoor market in Longdong University.

## 2.2 Preparation of nano Ag

In this typical experiment, 0.1 g soluble starch, 2~3 drops of  $0.05 \text{ mol} \cdot \text{L}^{-1}$  silver nitrate aqueous solution, 0.02 g dihydrate of trisodium citrate and 0.03 g glucose was successively put into 25 mL ultra-pure water in a small beaker and mixed evenly [6]. After the reaction, liquid was taken to test in a transparent tube and heated for 3 minutes until boiling in a household microwave oven. Finally, the buff nano Ag solution was successfully prepared.

## 2.3 Preparation of nano $\text{Fe}_3\text{O}_4$

At room temperature, 120 mL of  $1.5 \text{ mol} \cdot \text{L}^{-1}$  sodium hydroxide aqueous solution was put into a four-necked flask and then heated to  $80 \text{ }^\circ\text{C}$ .  $\text{Fe}_2(\text{SO}_4)_3 \cdot \text{XH}_2\text{O}$  (4.3 g),  $\text{Fe}_2\text{SO}_4 \cdot 7\text{H}_2\text{O}$  (1.5 g) and  $\text{H}_2\text{SO}_4$  (2 mL,  $2 \text{ mol} \cdot \text{L}^{-1}$ ) was mixed with 20 mL ultra-pure water thoroughly, and then the mixture was gradually dripped into NaOH solution at  $80 \text{ }^\circ\text{C}$  in the four neck flask to react for 1 h. Finally, magnetic  $\text{Fe}_3\text{O}_4$  nanoparticles were obtained through magnetic separation [7].

## 2.4 Preparation of Ag- $\text{Fe}_3\text{O}_4$ composites

Trisodium citrate aqueous solution ( $145 \text{ mL}$ ,  $11.0 \times 10 \text{ mol} \cdot \text{L}^{-1}$ ), sodium dodecyl benzene sulfonate aqueous solution ( $1 \text{ mL}$ ,  $0.7 \text{ mol} \cdot \text{L}^{-1}$ ) and the as-prepared magnetic  $\text{Fe}_3\text{O}_4$  nanoparticles ( $0.15 \text{ g}$ ) was put into a four-necked flask. While the mixed solution was heated to keep in a slightly boiling state,  $50 \text{ mL}$  of  $4 \times 10^{-2} \text{ mol} \cdot \text{L}^{-1}$  silver nitrate aqueous solution was quickly drop-wise added into the flask. Then the final mixture in the flask was mechanically stirred for 30 minutes. Finally, magnetic  $\text{Fe}_3\text{O}_4$ -Ag nanocomposite product was obtained by magnetic separation and dried in a vacuum [7].

## 2.5 Preparation of electrochemical sensors

The bare gold electrode was polished to mirror on chammy with  $0.3 \mu\text{m}$  and  $0.05 \mu\text{m}$   $\text{Al}_2\text{O}_3$  pasted and then treated ultrasonically in the secondary water to obtain a smooth electrode surface. Before the modification, the gold electrode was scanned in the mixture of potassium ferricyanide and potassium nitrate until a stable cyclic voltammogram was obtained. At the end of the experiment, the electrode must be ground clean, rinsed

with ultra-pure water and ethanol, dried and placed for next use [8-9].

A certain amount of dispersion solution of Ag- $\text{Fe}_3\text{O}_4$  nanoparticles was ultrasonicated for 2 minutes. The above solution ( $5 \mu\text{L}$ ) taken by the feeder was dripped onto the surface of the dried and pretreated bare gold electrode and dried naturally (or placed in a  $37 \text{ }^\circ\text{C}$  incubator) [10]. Then  $0.02 \text{ g}$  of chitosan (CHIT) was mixed with  $1 \text{ mL}$  of acetic acid solution evenly. Such mixture ( $5 \mu\text{L}$ ) was dripped onto the gold electrode modified with a solution of Ag- $\text{Fe}_3\text{O}_4$  nanoparticles and got dried in the air. Finally, an Ag- $\text{Fe}_3\text{O}_4$ /GCE chemical sensor was obtained.

## 2.6 Characterization

The morphology of the as prepared nanocomposite was identified with a JEOL JSM-6510LV and JEOL6700-F of scanning electron microscope (SEM) and transmission electron microscopy (TEM, FEI Tecnai G20). The ultraviolet-visible (UV-vis) diffuse reflectance spectra of the samples were obtained for the dry-pressed film samples by a UV-vis spectrophotometer (SPECORD50 PLUS, Analytik Jena).  $\text{BaSO}_4$  was used as a reflectance standard in a UV-vis diffuse reflectance experiment. In addition, the test instruments include electronic balance (BS110S), PHS-3C ray magnetic pH meter, PJ25B-A microwave oven, KQ3200 ultrasonic processing equipment, quartz UV cuvette, RST electrochemical workstation (Zhengzhou Cirusi instrument technology co., LTD.) and DHG-9140A electric thermostatic blast drying oven (Shanghai Yiheng technology co., LTD.).

## 3 Results and Discussion

The optical properties of the Ag- $\text{Fe}_3\text{O}_4$  composites were explored by UV-vis diffuse reflectance spectra (DRS).

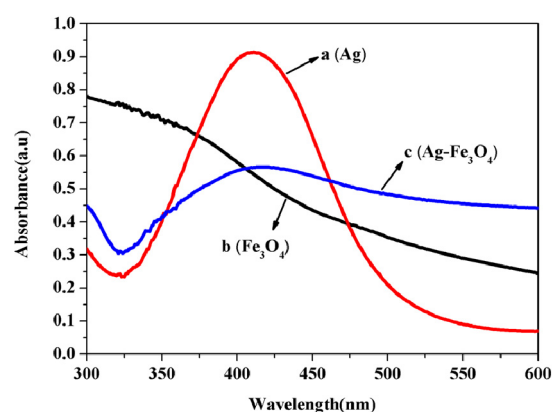


**Fig.1.** UV-vis DRS of (a) Ag (b) $\text{Fe}_3\text{O}_4$  nanoparticles (c) Ag- $\text{Fe}_3\text{O}_4$  composites.

Fig. 1 shows the UV-vis DRS of Ag,  $\text{Fe}_3\text{O}_4$  and Ag- $\text{Fe}_3\text{O}_4$  composites. The illustration shows that the absorbance of Ag nanoparticles at the wavelength of  $411 \text{ nm}$  was  $0.9126$  and the absorbance of the Ag- $\text{Fe}_3\text{O}_4$  nanoparticles at the wavelength of  $415 \text{ nm}$  was  $0.5661$ . The absorption edge of the Ag- $\text{Fe}_3\text{O}_4$  was shifted to a longer wavelength compared with that of pure Ag due to

the contribution of black Fe<sub>3</sub>O<sub>4</sub>. Therefore, the observation in the UV-Vis diffuse reflectance spectra indicates that Ag nanoparticles were successfully coated on the surface of Fe<sub>3</sub>O<sub>4</sub> particles.

The microscopic morphologies of Ag-Fe<sub>3</sub>O<sub>4</sub> composites and pure Fe<sub>3</sub>O<sub>4</sub> nanoparticles were determined by scanning electron microscopy (SEM) and transmitting electron microscopy (TEM). The pure Fe<sub>3</sub>O<sub>4</sub> nanoparticles were investigated. As shown in Fig.2(b,c), Fe<sub>3</sub>O<sub>4</sub> is distinct from lattice fringes. However, because of the magnetic effect, Fe<sub>3</sub>O<sub>4</sub> nanoparticles were easily agglomerated and difficult to disperse evenly in water. Fig 2(a,b) shows a typical SEM image of Ag-Fe<sub>3</sub>O<sub>4</sub> composites which was composed of irregular small blocks, and the surface was attached with many small particles. The TEM image further confirms this phenomenon. As shown in Fig 2(d,e), the Ag-Fe<sub>3</sub>O<sub>4</sub> composite nanoparticles resemble the core-shell, and the surface of Fe<sub>3</sub>O<sub>4</sub> was coated with a layer of silver particles and dispersed more evenly. It can be found that the Ag nanoparticles effectively inhibited the agglomeration of the magnetic Fe<sub>3</sub>O<sub>4</sub> nanoparticles and improved the stability of these nanoparticles.

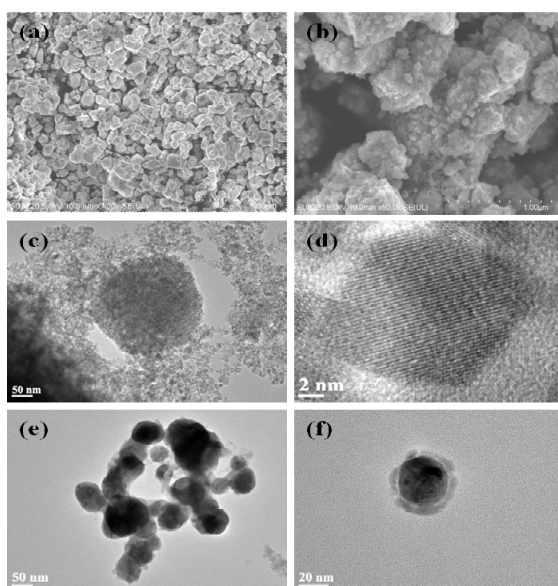


**Fig.2.** (a), (b)SEM image of Ag-Fe<sub>3</sub>O<sub>4</sub> nanoparticles; (c), (d) TEM image of Fe<sub>3</sub>O<sub>4</sub> nanoparticles; (e), (f) TEM image of Ag-Fe<sub>3</sub>O<sub>4</sub> composites.

With the Ag-Fe<sub>3</sub>O<sub>4</sub>/GCE as working electrode, the saturated calomel electrode (SCE) as reference electrode, platinum wire electrode as counter electrode, different concentrations of methomyl with phosphate buffer solution (0.1 mol·L<sup>-1</sup>, pH=6.9) were scanned several times through cyclic voltammetry for detecting the electrochemical properties of different concentrations of methomyl. Until the curve was stable, the cyclic voltammogram was obtained to record peak current and corresponding potential. Fig.3 is the cyclic voltammogram obtained by a scanning concentrations of 2.97 × 10<sup>-5</sup> mol·L<sup>-1</sup> ~ 3.47 × 10<sup>-4</sup> mol·L<sup>-1</sup> methomyl. It has been found that when the concentration of methomyl was 1.04 × 10<sup>-4</sup> mol·L<sup>-1</sup>, its electrochemical performance is optimal.

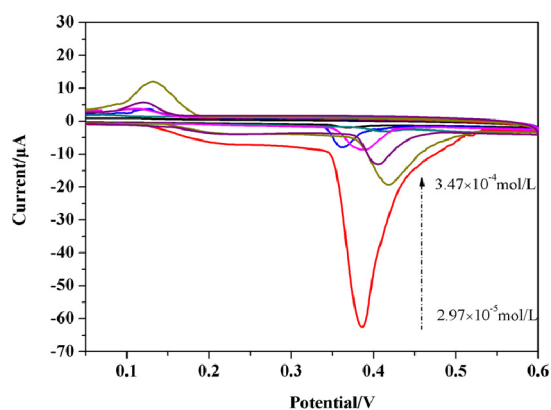


**Fig.3.** Cyclic voltammetry of different concentrations of methomyl.

### 3.1 Conditional optimization experiment

The effect of pH value of phosphate buffer solution on the peak current response of Ag-Fe<sub>3</sub>O<sub>4</sub>/GCE electrode was studied in this experiment. When the pH value of phosphate buffer solution was 6.0 to 7.0, the peak current of Ag-Fe<sub>3</sub>O<sub>4</sub>/GCE chemical sensor in the concentration of 1.04 × 10<sup>-4</sup> mol·L<sup>-1</sup> methomyl prepared with phosphate buffer solution was measured to find the optimal pH value of phosphate buffer solution. The peak current value of the buffer solution was optimum at a pH value of 6.85 to 7.0 (Fig.4). Carbamate pesticides were relatively stable in acidic environment and easily decomposed when exposed to alkalis, so the pH value of 6.9 was chosen as the acidity of this experiment [11].

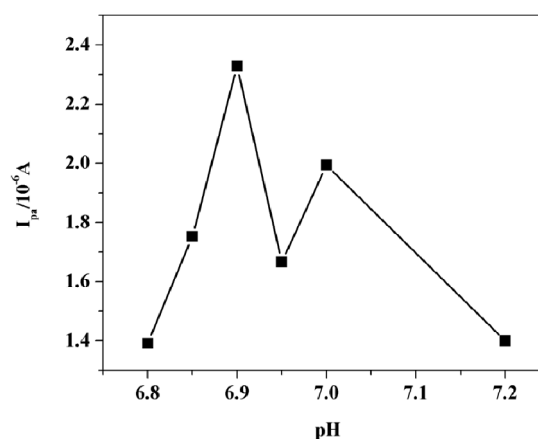


**Fig.4.** Effect of pH on the amperometric response of the sensor to 1.04 × 10<sup>-4</sup> mol·L<sup>-1</sup> methomyl.

During the modification of the Ag-Fe<sub>3</sub>O<sub>4</sub>/GCE electrode, the effect of the Ag-Fe<sub>3</sub>O<sub>4</sub> nanoparticle solution dosage on the peak current response of this electrode was discussed in this experiment. When the dosage of solution was 3~15 µL, the peak current of Ag-Fe<sub>3</sub>O<sub>4</sub>/GCE chemical sensor in a series of values selected were measured respectively at a pH value of 6.9 and a concentration of 1.04 × 10<sup>-4</sup> mol·L<sup>-1</sup> methomyl, and the optimum amount of modification was determined. When less Ag-Fe<sub>3</sub>O<sub>4</sub> nanoparticles were immobilized on the electrode, the response current was small, and maybe too small to completely react with methomyl, so the

response was not sensitive enough (Fig.5). With the increment of coating drops, the peak current value became larger and reached the maximum at 5  $\mu\text{L}$ . When the amount of coating drops continued to increase, the response current tended to decrease because the drop coating was too thick, which caused greater resistance. After reaching 8  $\mu\text{L}$ , it started to increase again, and the effect of the resistance was negligible. After reaching 8  $\mu\text{L}$  coating drops, the peak current value increased, but the surface of the electrode was very limited. When the amount of coating was too large in the dispensing, there was partial loss and the measurement was inaccurate. Therefore, 5  $\mu\text{L}$  of the modification coating drops was selected in this experiment appropriately.

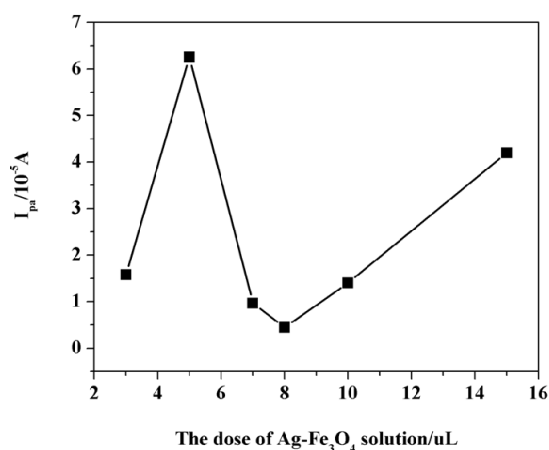


**Fig.5.** Effect of modifier on the amperometric response of the sensor to  $1.04 \times 10^{-4} \text{ mol} \cdot \text{L}^{-1}$  methomyl.

The scan rate had a great influence on the peak current. A good linear relationship was presented between the reduction peak current and the square root of scan rate within a certain range (Fig.6). Therefore, the linear regression equation was  $I = 13.48 - 70.72V^{1/2}$ , and the linear coefficient R was 0.9967. It shows that the mass transfer process of the electrode was controlled by diffusion. When the scan rate was too high, the background current became larger and could interfere the measurement of peak current. In this experiment, 0.1 V/s was taken as the optimal scan rate with the best signal-to-noise ratio [12-13].

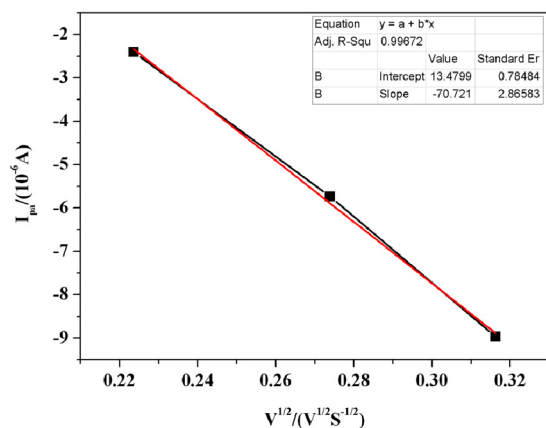


**Fig.6.** Effect of scan rate on the amperometric response of the sensor to  $1.04 \times 10^{-4} \text{ mol} \cdot \text{L}^{-1}$  methomyl.

Under optimized experimental conditions, the methomyl solution diluted 100 times was further diluted 35 times, 50 times, 100 times, 150 times, 200 times, 250 times, 300 times, and 350 times for tests. (The concentration of methomyl stock solution was  $1.04 \text{ mol} \cdot \text{L}^{-1}$ ). Different peak currents at different concentrations of methomyl were measured experimentally to obtain a working curve for methomyl pesticides (Fig.7).  $I = 0.3973C + 0.412$  ( $C$  was  $1.04 \times 10^{-4} \text{ mol} \cdot \text{L}^{-1}$ ),  $R^2 = 0.9903$ .

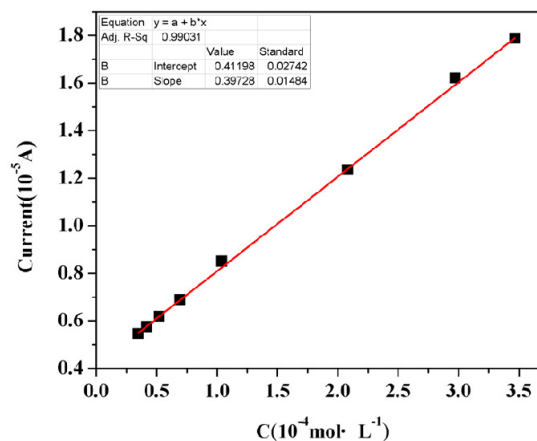


**Fig.7.** Current response of electrodes at different concentrations.

### 3.2 Sample determination

The edible part of lettuce, oilseed rape and spinach was selected and cut into pieces with a knife, and then accurately weighed 10 g into two erlenmeyer flasks. Phosphate buffer solution (50 mL) was added in one erlenmeyer flask, and acetone (5 mL) and phosphate buffer solution (45 mL) was added in other erlenmeyer flask. After soaking shreds for about 12 h, the soaked liquid was followed by the sonication for 5 minutes. Then the liquid was stood for a while. Finally, the supernatant was poured out for further use.

The liquid phase of lettuce (1.0 mL), oilseed rape (2.5 mL), and spinach (5 mL) respectively was transferred into a volumetric flask in turn. Under the optimized experimental conditions, added phosphate buffer to scale respectively. Finally, added the standard solution of methomyl, measured 3 parallel tests, took the average value and calculated the recovery rate.

The peak currents of the above samples (1 mL of lettuce test solution, 2.5 mL of oilseed rape test solution, and 5 mL of spinach test solution) were measured in parallel for 3 times by cyclic voltammetry to compare with the above standard curve, and then the residual amount of their pesticide was obtained. It was calculated that the pesticide concentration in spinach, oilseed rape and lettuce was respectively  $0.1099 \times 10^{-4} \text{ mol} \cdot \text{L}^{-1}$ ,  $0.4996 \times 10^{-4} \text{ mol} \cdot \text{L}^{-1}$  and  $0.4276 \times 10^{-4} \text{ mol} \cdot \text{L}^{-1}$ . The standard addition method was used to estimate the accuracy of this method. After adding  $1.04 \times 10^{-4} \text{ mol} \cdot \text{L}^{-1}$  methomyl standard solution into the test solution, its peak current value was  $4.9131 \times 10^{-6} \text{ A}$ . Then the average value of 3 parallel tests was taken and the recovery rate

was calculated. {recovery rate=[(standard sample test value - sample test value) / (the adding standard amount)] $\times$ 100%}. The results are shown in Table 1.

**Table 1.** The determination of results of vegetable sample(n=3).

vegetable samples	non-standard sample I <sub>0</sub>	standard sample I	recovery rate
lettuce	5.8176	10.293	91.09%
oilseed rape	6.1033	10.534	90.02%
spinach	3.6824	8.5101	98.26%

From the recovery rates in Table 1, it could be seen that methomyl was completely recovered by this method, so it was feasible for detection the methomyl residuals.

### 3.3 Measurement of interference experiment

This experiment investigated the interference of three organophosphorus pesticides on methomyl. 1 mL stock solution of each of the three pesticides of dichlorvos, chlorpyrifos and phoxim was diluted 5,000 times, and then added into  $1.04 \times 10^{-4}$  mol $\cdot$ L<sup>-1</sup> of methomyl standard solution. The peak current value of the above solution was measured through cyclic voltammetry to compare with the standard solution [14]. Experiment results show that dichlorvos, chlorpyrifos and phoxim would interfere with the determination of methomyl.

## 4 Conclusions

In this method, a new electrochemical sensor Ag-Fe<sub>3</sub>O<sub>4</sub>/GCE was prepared, and the electrode response of this sensor to different concentrations of methomyl solution was determined in a phosphate buffer solution with a pH value of 6.9. The pesticide residues of methomyl in vegetables determined by this sensor was used to establish a method for the determination of carbamate pesticides in agricultural products. It is simple, fast, responsive, low sample dosage and non-destructive to the samples, and it may have broad development prospects in the future.

## Acknowledgement

This research was financially supported by Gansu Provincial Science and Technology (Sci & Tech) Department Small and Medium Enterprises (SME) Innovation Fund (Project Nos. 1604JCCM126).

## References

1. Lu Y H, Chen Y J, Zou L H et al, Determination of methomyl residues in vegetables by high performance liquid chromatography, *Chin. J. Prev Med*, **28**(1994):175-176
2. Tan Y Y, Niu M, Tian H, Determination of six kinds of carbamate pesticides in vegetables and mushrooms by solid phase extraction coupled with

- gas chromatography-mass spectrometry, *J. In. Quar*, **27**(2017):10-13
3. RZW·Wufuli, Application of spectrophotometry on the determination of pesticides residues in vegetables, *Rural Sci. Tech.· Clay Fer. Plant Prot*, **12**(2016):76
4. Yin J J, Discussion of chemiluminescence technology on the determination of pesticides residues, *Rural Econ. Sci Tech*, **27**(2016):127,173
5. Zhang B H, Wei W, Study on the effect of enzyme inhibition method for determination of pesticide residues in vegetables, *S Chin Agri*, **12**(2018):105-106
6. Luo P, Preparation of silver nanoparticles by starch, *Chem. Teac*, **2**(2016):60-62
7. Liu J M, Liu W H, Teng Y J et al, Adsorption of oxamyl on Fe<sub>3</sub>O<sub>4</sub>-Ag magnetic nanoparticles surface with surface-enhanced raman scattering, *Spectrosc Spec Anal*, **37**(2017):2061-2066
8. Shan Y J, Wu G F, Lu X Q et al, Studies on the copper ion imprinting sensors based on the gold nanomaterials, *Chem Res. Appl*, **29**(2017):786-792
9. Hong M, Qu Y H, Li X H et al, Au-doped Fe<sub>3</sub>O<sub>4</sub> nanoparticle immobilized acetyl cholinesterase sensor for the detection of organophosphorus pesticide, *Acta Chim Sinica*, **20** (2007):2303-2308
10. Liu Y J, Wu L S, Shi Z et al, Sensitive electrochemical response and analysis of parathion at SWNT/Au-Fe<sub>3</sub>O<sub>4</sub> modified electrode, *Chin J. Anal Lab*, **31**(2012):21-25
11. Wang J, Chen R, Guo C et al, Determination of 16 carbamate pesticides and metabolite residues in plant-derived foodstuffs by high pressure liquid chromatography-tandem mass spectrometry, *J. Food Saf. Qual*, **4**(2013):1458-1466
12. Wu M, Study on nano-materials modified electrochemical sensors and their application in harmful substances detection, *Dissertation, E Chin Norm U*, (2014)
13. Zhai Y M, Zhai J F, Wang Y L et al, Fabrication of iron oxide core/gold shell submicrometer spheres with nanoscale surface roughness for efficient surface-enhanced raman scattering, *J.Phys. Chem.C*, **113**(2009):7009-7014
14. Chen H S, Zhang X L, Cui C J, Research progress on electrochemical sensor in the way of heavy mental detection, *Food Res. Develop*, **37**(2016):205-208